



# Improved opto-electrical properties of spray deposited ytterbium doped cadmium oxide thin films

S. P. Desai<sup>1</sup>

Received: 21 May 2018 / Accepted: 27 June 2018 / Published online: 30 June 2018  
© Springer Science+Business Media, LLC, part of Springer Nature 2018

## Abstract

Transparent conducting metal oxides (TCOs) associate the properties of high optical transparency and electrical conductivity, which makes them suitable for variety of applications such as window layer in liquid crystal and electroluminescent display devices as well as in solar cells. Among different TCO's, cadmium oxide (CdO) has received tremendous attention as a potential alternative to Sn-doped  $\text{In}_2\text{O}_3$  (ITO) due to its high intrinsic dopability coupled with outstanding mobility and high electrical conductivity. In the present study, for first time the doping of ytterbium (Yb) into CdO films prepared using a simple and effective spray pyrolysis technique demonstrated. The structural, morphological and optoelectronic properties of Yb doped CdO thin films as a function of Yb concentration (1–3 at.%) have been studied. X-ray diffraction, field-emission scanning electron microscopy, X-ray photoelectron spectroscopy, optical absorption spectroscopy, luminescence measurements and for electrical properties Hall effect set up in van der Pauw configuration have been employed to study the properties of Yb-doped CdO thin films. Yb doped CdO thin films exhibit excellent optical transparency, with an average transmittance over 75% in the visible region. It is found that Yb doping widens the optical band gap from 2.63 to 2.88 eV, via a Moss–Burstein shift and further decreases to 2.77 eV. The maximum reflectivity of 97.24% achieved for 2.5 at.% Yb:CdO film. The better values of resistivity, carrier concentration, mobility and figure of merit have been obtained for 2.5 at.% Yb:CdO, which are  $2.6 \times 10^{-4} \Omega \text{ cm}$ ,  $13.9 \times 10^{20} \text{ cm}^{-3}$ ,  $17.39 \text{ cm}^2/\text{Vs}$  and  $45.87 \times 10^{-3} (\Omega)^{-1}$  respectively. The obtained results revealed that Yb dopant has a significant influence on the optoelectronic properties of CdO-based TCO compound.

## 1 Introduction

Transparent conducting oxides (TCO's) are both optically transparent and electrically conductive, which are extensively used in optoelectronic devices such as flat panel displays, organic light emitting diodes, photovoltaics, heat reflectors, energy efficient windows etc. [1–5]. Cadmium oxide (CdO) based TCO's have received much attention due to their exceptional carrier concentrations, good conductivities and relatively simple cubic rocksalt crystal structure [6]. CdO thin films have high transparency (> 75%) in the visible region of the electromagnetic spectrum and show degenerate n-type conductivity mainly due to oxygen vacancies and Cd interstitials as well as high carrier concentration of about  $10^{20}/\text{cm}^3$  and high electrical conductivity ( $10^2$ – $10^4 \text{ S/cm}$ ) contributed by shallow donors resulting

from self non-stoichiometry. CdO contains broadly dispersed s-like conduction bands and a small carrier effective mass ( $0.21 \pm 0.01 m_0$ ), which represent an ideal material to study the effects of doping on TCO band structure, crystal chemistry and charge transport. The optical band gap of undoped bulk CdO is 2.3 eV, leading to relatively poor optical transparency in the short wavelength range, which makes it less desirable [7]. However, doping offers the possibility of tuning the electronic structure and the optical band gap through a carrier concentration dependent Moss–Burstein (MB) energy level shift and its low effective carrier mass allows efficiently increasing the band gap of heavily doped CdO films to as high as 3.35 eV [8]. Dhakel [9–14] has extensively studied the effect of different dopants like Eu, Sm, Ga, Tl, Fe, Gd etc. on the structural and opto-electrical properties of CdO thin films deposited by vacuum evaporation technique. It has been reported that the ionic radius and the properties of doped ions changes the electrical and optical properties of CdO thin films. The variation in band gap is explained by the bandgap narrowing and widening effect based on MB effect.

✉ S. P. Desai  
swayamswaraj@gmail.com

<sup>1</sup> Department of Basic Sciences and Humanities, KITs College of Engineering, Kolhapur, MS 416234, India

Undoped CdO and doped CdO films with good structural, electrical and optical qualities have been reported from a variety of techniques such as reactive evaporation [15], solution growth [16], sputtering [17], spray pyrolysis technique (SPT) [18], chemical bath deposition [19] and metal organic chemical vapor deposition [20] and pulsed laser deposition [21]. Among these techniques, a simple SPT offers several advantages over techniques such as easy and low-cost equipment design, and amenability for large area thin film fabrication with high throughput, homogenous coverage and easy control over growth chemistry of doping impurities. In our previous studies, CdO thin films have been grown successfully using SPT and different preparative parameters like temperature, thickness etc have been optimized. It is found that the CdO film with thickness of 1371 nm, deposited at 350 °C substrate temperature exhibited the highest transmittance of 74%, figure of merit of  $18.23 \times 10^{-3} (\Omega)^{-1}$ , carrier concentration of  $7.30 \times 10^{20}/\text{cm}^3$  and mobility of  $23.11 \text{ cm}^2/\text{Vs}$  [22].

The paper deals with the preparation of Yb doped CdO thin films by SPT for the first time and its effect on the different physico-chemical as well as optoelectrical properties have been studied.

## 2 Experimental details

### 2.1 Yb:CdO thin film preparation

CdO thin films were prepared using SPT using our previously reported recipe [6]. For Yb doping, stock solution of 0.1 M ytterbium nitrate ( $\text{YbNO}_3$ ) was prepared in double distilled water (DDW) and mixed in appropriate volume (for 40 ml spray solution) for achieving particular doping concentration (1, 1.5, 2, 2.5 and 3 at.%) in aqueous solution of 0.1 M cadmium acetate dihydrate  $\text{Cd}(\text{CH}_3\text{COO})_2 \cdot 2\text{H}_2\text{O}$ . The deposition parameters like substrate temperature (350 °C), spray rate (4 ml/min), nozzle to substrate distance (30 cm), pressure of carrier gas ( $75 \text{ kg}/\text{cm}^2$ ) and quantity of spraying solution (40 ml) were kept constant. It has been observed that when solution is sprayed on preheated glass substrate, pyrolytic decomposition of solution takes place and yellowish brown color films formed. These films were then allowed to cool at room temperature and were further used for structural, morphological, compositional, chemical, optical, electrical and luminescent characterization.

### 2.2 Characterization

The structural properties were studied by X-ray diffractometer [Bruker AXS (D2-Phaser) USA] using  $\text{Cu K}\alpha$  ( $\lambda = 1.5406 \text{ \AA}$ ) operated at 30 kV, 20 mA. The microstructural study was carried out using field emission scanning

electron microscopy (FE-SEM) [Hitachi S-4800, Japan]. The thickness of the thin films was obtained from the cross sectional FE-SEM images. The elemental composition in deposited film was verified by using energy dispersive X-ray analysis (EDAX) attached with FE-SEM, X-ray photoelectron spectroscopy (XPS) [Kratos Analytical, ESCA 3400, UK] study was carried out to confirm chemical composition as well as their different energy states. The transmission and optical absorption spectra were studied at room temperature within 200–800 nm wavelength range using UV–Vis spectrophotometer [Shimadzu UV-1800, Japan]. The room temperature electrical measurements were carried out with Hall Effect set up in van-der Pauw configuration [SES Instruments Pvt. Ltd. Roorkee, India]. The photoluminescence spectra were recorded using spectrofluorometer [Fluoromax-4, Japan].

## 3 Results and discussion

### 3.1 X-ray diffraction (XRD) study

The detailed knowledge of internal structure of crystal has been obtained from XRD study. When X-rays of suitable wavelength made incident on the crystal, diffraction of X-rays takes place from periodic array of atoms or molecules which acts like scattering centers and form crystal planes separated by distance of the order of wavelength of X-ray. It is one of the suitable techniques for characterizing the microstructure of the thin films. Presence and composition of phases, grain size, orientation of crystallites, strain and dislocation density etc. obtained from XRD data. The XRD patterns of Yb doped CdO (Yb:CdO) thin films deposited with different (1–3 at.%) Yb doping concentration is shown in Fig. 1. Two prominent diffraction peaks are observed in the XRD patterns, which can be indexed to (111) and (200) planes along with these minor peaks are also observed which are indexed to (220), (311) and (222) indicating the phase pure face centered cubic (FCC) structure of Yb:CdO films [JCPDS Card No. 01-075-0592] [6]. The intensity of (200) plane is higher than all other planes for all the Yb:CdO films. No any observable impurity peaks have been found in XRD patterns suggesting that  $\text{Cd}^{2+}$  ions are successfully substituted by  $\text{Yb}^{2+}$  ions in CdO lattice. The crystallite size of different planes is estimated using the Scherrer's equation [22]. The calculated average crystallite size for 1–3 at.% Yb:CdO films are found to be 34.19, 35.10, 40.24, 48.94, and 34.32 nm respectively and presented in Table 1. The crystallite size varies with doping concentration of Yb which may be due to occupation of Yb atoms at regular sites in the CdO lattice, or the decrease in crystallite size at higher Yb doping concentration (3 at.%) is may be due to increase in nucleation sites with Yb doping or due to the saturation of Yb over CdO samples, which is correlated to the FE-SEM

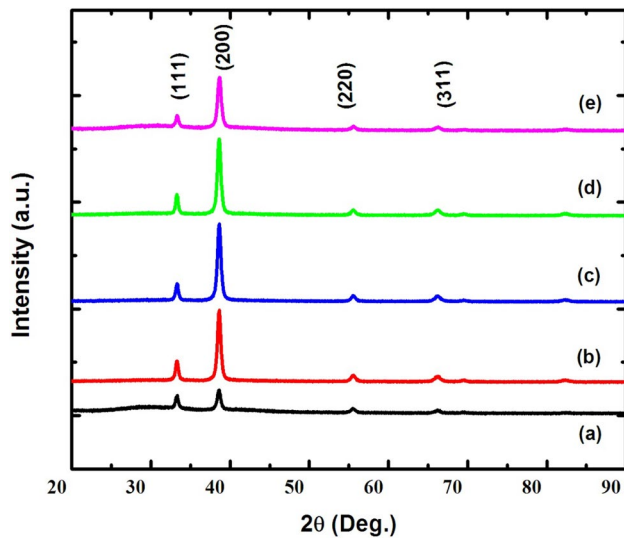


**Fig. 1** The XRD of Yb:CdO thin films of different Yb doping concentration (a) 1 at.%, (b) 1.5 at.%, (c) 2 at.%, (d) 2.5 at.% and (e) 3 at.%, deposited at optimized substrate temperature of 350 °C

micrographs [23]. It is observed that the intensity of XRD peak along (200) plane increase with doping concentration of Yb which is due to the higher growth rate of film along x-axis

and it can also attributed to the minimum surface energy along this direction.

Crystalline quality of the film can also be determined by analyzing the dislocation density; it gives the amount of defects available in the deposited films. The dislocation density ( $\delta$ ), defined as the length of dislocation lines per unit volume, has been estimated using the following formula [8]

$$\text{The dislocation density, } (\delta) = \frac{n}{D^2} \quad (1)$$

where D is crystallite size and n is factor which equals unity giving minimum dislocation density. The calculated values of  $\delta$  are given in Table 1. It is observed that the values of  $\delta$  varies non-linearly, as it depends on the variation of crystallite size. The dislocation density calculated for 1–3 at.% Yb:CdO films are  $8.55 \times 10^{14}$ ,  $8.11 \times 10^{14}$ ,  $6.17 \times 10^{14}$ ,  $4.17 \times 10^{14}$  and  $8.48 \times 10^{14}$  lines/m<sup>2</sup>. The minimum dislocation density is observed for 2.5 at.% Yb:CdO film.

It is also observed from Fig. 1 that the preferred orientation of Yb:CdO thin films is along x-axis perpendicular to the substrate orientation, which is evidenced from highly textured (200) plane. The texture coefficient (TC) for preferred orientation of plane is calculated using following expression [24]

$$TC_{(hkl)} = \frac{\frac{I_{(hkl)}}{I_{0(hkl)}}}{\frac{1}{N} \sum \frac{I_{(hkl)}}{I_{0(hkl)}}} \quad (2)$$

**Table 1** The values of Bragg's angle ( $2\theta$ ), Miller indices (hkl), texture coefficient (TC), lattice constant (a), crystallite size (D), strain ( $\epsilon$ ) and dislocation density ( $\delta$ ) of 1–3 at.% Yb:CdO films deposited at 350 °C on SLG substrate

Yb:CdO (at.%)	$2\theta$ (°)	Miller indices (hkl)	Texture coeff. TC	Lattice constant a (Å)	Crystallite size D (nm)	Avg. D (nm)	Strain $\epsilon \times 10^{-2}$	Dislocation density $\delta \times 10^{14}$ (lines/m <sup>2</sup> )
1	33.13	111	1.39	4.68	60.17	34.19	2.38	8.55
	38.59	200	2.37	4.66	26.72			
	55.46	220	0.49	4.68	32.58			
	66.30	311	0.351	4.67	17.20			
1.5	33.27	111	1.32	4.66	52.64	35.10	3.14	8.11
	38.53	200	3.65	4.66	21.38			
	55.41	220	0.325	4.68	45.60			
	66.30	311	0.386	4.67	20.08			
2	33.34	111	1.03	4.65	46.80	40.24	0.96	6.17
	38.62	200	3.97	4.66	28.49			
	55.51	220	0.314	4.68	45.57			
	66.16	311	0.366	4.68	40.11			
2.5	33.24	111	0.941	4.66	70.19	48.94	0.71	4.17
	38.48	200	4.11	4.67	87.65			
	55.36	220	0.291	4.69	20.72			
	66.05	311	0.342	4.69	17.21			
3	33.23	111	1.17	4.66	57.56	34.32	2.13	8.48
	38.6	200	3.86	4.66	20.62			
	55.56	220	0.301	4.67	46.76			
	66.17	311	0.35	4.67	12.34			

where  $I$  is the intensity of (hkl) plane,  $I_0$  is the corresponding plane intensity from JCPDS data Card No. 01-075-0592 and  $N$  is the total number of XRD peaks obtained. From TC values measured for various planes for undoped and Yb:CdO thin films, it is clear that all films have preferential orientation along (111) and (200) planes. The maximum TC values for the (200) planes are found to be 2.37, 3.65, 3.97, 4.11 and 3.86 for the Yb:CdO films. It is observed that 2.5 at.% Yb:CdO films show maximum TC value of 4.11 amongst all the Yb:CdO films.

The lattice constants calculated for (111) planes are 4.68, 4.66, 4.65, 4.66 and 4.66 Å and (200) planes are 4.66, 4.66, 4.66, 4.67 and 4.66 Å. The average lattice constant ( $a$ ) calculated for (111) planes and (200) plane is same that is 4.662 Å, which is slightly less than standard lattice constant of CdO film (4.69 Å) compared to JCPDS Card No. 01-075-0592, the slight deviation in lattice constant found for these planes as depicted in Table 1, which is responsible for developing strain in the Yb:CdO thin film. Generally, strain in the films generated due to interlayer lattice mismatch during the growth of the film, deficiencies and defect generated in film like edge dislocation, screw dislocation and void spaces etc. because of which unit cell of crystal structure gets deformed resulting in developing strain. The strain in the sample is determined by using the equation [25]

$$\beta = \frac{\lambda}{D \cos \theta} - \varepsilon \tan \theta \quad (3)$$

where  $\beta$  is full width at half maximum,  $\lambda$  is the wavelength of X-ray,  $D$  is the crystallite size,  $\theta$  is the Bragg's angle and  $\varepsilon$  is the strain in film. It is seen that strain decreases with increase in Yb doping concentration in CdO thin films and their values are depicted in Table 1. The maximum strain is of  $3.14 \times 10^{-2}$  observed for 1 at.% Yb:CdO thin film and it decreases with increase in Yb doping to  $0.71 \times 10^{-2}$  for 2.5 at.% Yb:CdO film whereas again it increases to  $2.13 \times 10^{-2}$  for 3 at.% Yb:CdO, The reduction of strain may be due to the improvement in crystallinity. Such kind of nature can also be explained based upon thickness, nature of crystallinity, crystal size variation, TC and variation in lattice constant. From the various structural parameters obtained, it is found that CdO film doped with 2.5 at.% Yb doping shows better results and hence 2.5 at.% Yb doping is optimized doping concentration.

### 3.2 Field emission scanning electron microscopy (FE-SEM) studies

Surface morphology and film thickness are examined by FE-SEM images and are presented in Fig. 2. All the Yb:CdO thin films shows homogenous, crack free, compact morphology which confirms uniform growth of film during pyrolytic decomposition. Figure 2 shows the microstructure of

the Yb:CdO thin films changes with increasing Yb doping concentration. The 1 at.% Yb:CdO FE-SEM images shows that somewhat spherical, peanut like interconnected crystallite on the first layer of film is formed with few voids. The 1.5 at.% Yb:CdO has same double layered structure with upper layer showing more uniformity, cluster and crowded grains compared to films deposited with 1 at.% Yb, also very less number of voids are seen on its surface. With increase in Yb concentration it is observed for 2 at.% Yb:CdO film compact structure, mixture of small and larger grains are seen with almost no voids in the surface. 4 at.% Yb:CdO film show better uniform, compact and void free structure with undistinguished grain boundaries. Further the 3 at.% Yb:CdO film seems to be flat with no significant grain boundaries, it may be due to more thickness of this film. The cross-sectional FE-SEM images are used for measurement of thickness of Yb:CdO thin films. The film thickness increases with increase in Yb doping concentration in CdO thin film. The thickness of the Yb:CdO film are 746, 897, 1143, 1375 and 1562 nm for 1, 1.5, 2, 2.5 and 3 at.% Yb doped CdO thin films respectively. The increase in thickness of Yb:CdO film is attributed to the increased Yb concentration and larger growth rate of film.

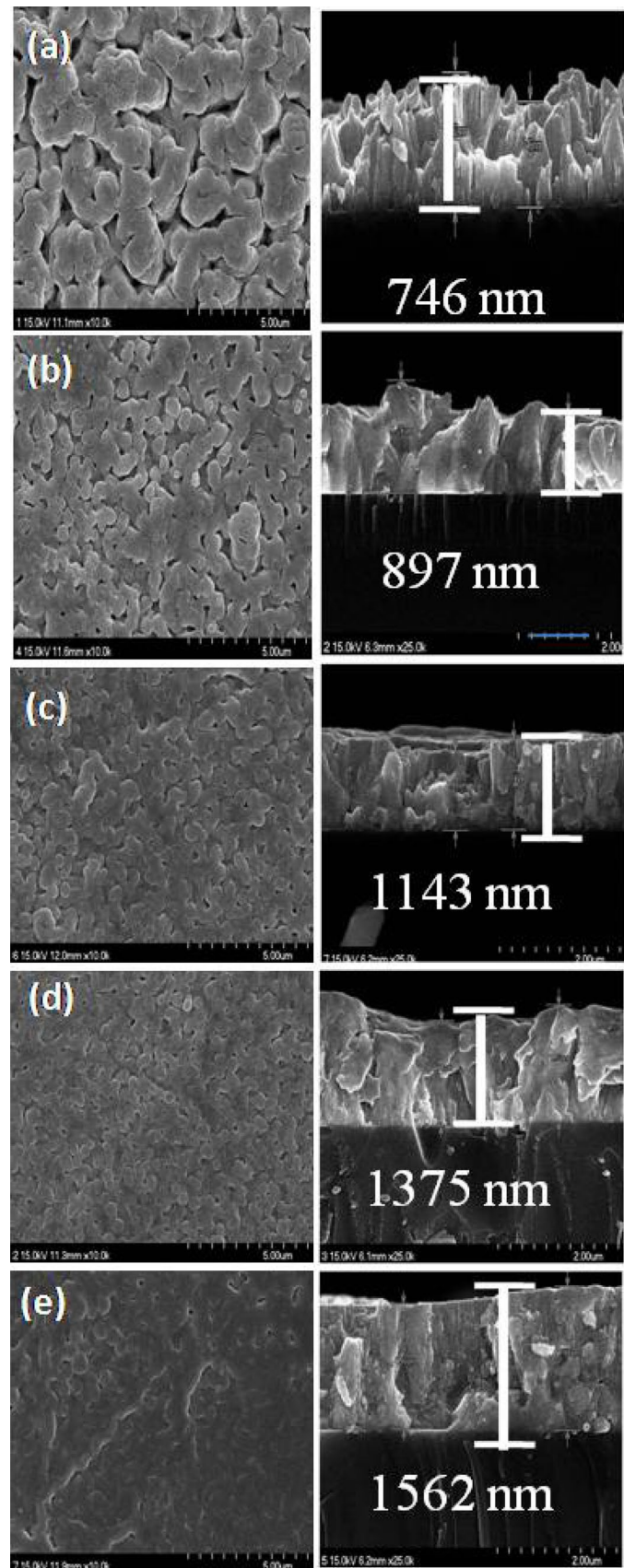
### 3.3 Energy dispersive X-ray analysis (EDAX) studies

Figure 3 shows the EDAX spectra of typical 2.5 at.% Yb:CdO thin film deposited at temperature 350 °C on SLG substrate which shows that the main compositions of the Yb:CdO films are Cd, O and Yb. It is further confirmed from XPS results obtained. The atomic percentages of Cd, O and Yb in the films are found as 56.03, 42.50 and 1.48 at.% respectively, indicating that they are composed of nearly sub-stoichiometric Yb:CdO thin films. The O/Cd ratio obtained from EDAX result is 0.75 suggesting that the film is having oxygen deficiency which is one of the factor responsible for improved opto-electrical properties of Yb:CdO film.

### 3.4 X-ray photoelectron spectroscopy (XPS) studies

The survey scan XPS spectra of the typical 2.5 at.% Yb:CdO thin film deposited at 350 °C substrate temperature is shown in Fig. 4. The chemical composition of the materials is determined using area under the curve of peaks. Using this, ratio of the O/Cd is calculated and it is found  $< 1$  ( $\sim 0.85$ ) that confirms the typical Yb:CdO thin film is sub-stoichiometric in nature. Photoelectron peaks observed at 10.77, 69.42, 405, 411.5, 620 and 652.6 eV corresponds to 4d, 4s, 3d<sub>5/2</sub>, 3d<sub>3/2</sub>, 3p<sub>3/2</sub>, 3p<sub>1/2</sub> fine structure states of Cd, respectively, whereas peaks at 773 and 975.18 eV belongs to the Auger electron peaks of Cd and O, respectively [26]. Along with this, peak at binding energy 284.46 eV is of 1s core level

**Fig. 2** The surface and cross-sectional FE-SEM images of Yb:CeO thin films of different Yb concentration deposited at 350 °C substrate temperature



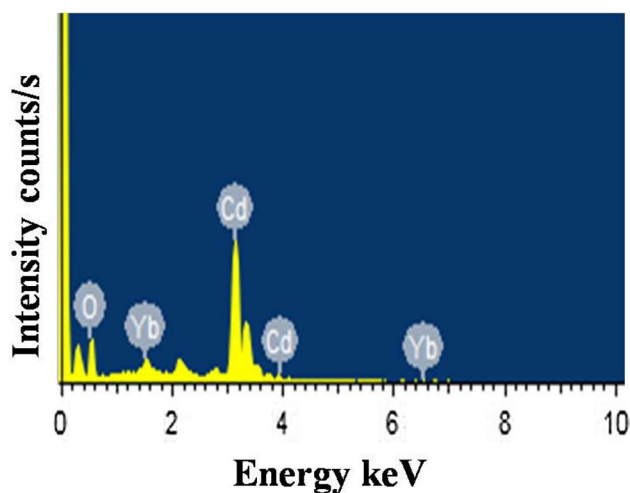


Fig. 3 EDAX spectra of typical 2.5 at.% Yb:CdO film

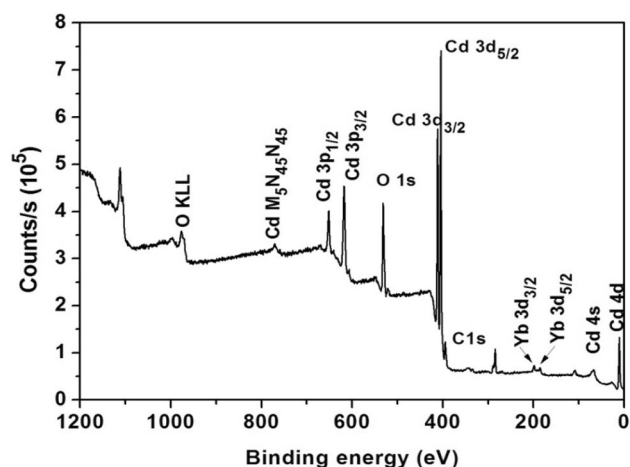


Fig. 4 XPS spectra of 2.5 at.% Yb:CdO thin film deposited at optimized substrate temperature of 350 °C

of carbon. The presence of carbon is due to contamination which resulted from the sample handling and exposing to air before the XPS measurement. Peak at 532 eV is attributed to the oxygen 1s fine structure state. Except s state p, d, f states splits into the doublet. Splitting is due to the presence of electrons with different spin-orbit coupling which usually having different binding energies indicating different fine structure states. The peak at 186.71 and 199.74 eV corresponds to the  $3d_{5/2}$  and  $3d_{3/2}$  states of Yb, respectively.

Detailed narrow scan XPS spectrum of the 3d core level of Cd is shown in Fig. 5 Electron orbit splitting of core level into doublet is due to spin orbit coupling of electrons. Observed spectrum is deconvoluted into two doublets lying at different energy levels. Two doublets belong to the two different chemical states of the Cd viz.  $Cd^{1+}$  and  $Cd^{2+}$ .

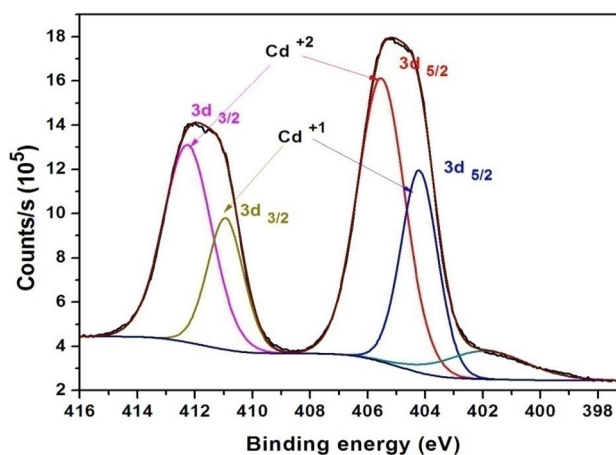


Fig. 5 Narrow scan spectra of 2.5 at.% Yb:CdO thin film deposited at optimized substrate temperature of 350 °C

Intense doublet lying at 405.05 and 411.75 eV corresponds to the  $3d_{5/2}$  and  $3d_{3/2}$  core levels of Cd due to the  $Cd^{2+}$  chemical state. Photoelectron peaks lying at binding energy 403.19 and 409.96 eV corresponding  $3d_{5/2}$  and  $3d_{3/2}$  core levels of Cd due to the  $Cd^{1+}$  chemical state. Area under the curve determines concentration of the corresponding chemical state of the element. Thus it could be concluded that the concentration of the  $Cd^{1+}$  valence state is less as compared with the  $Cd^{2+}$  state. The area under the curve is measured, and the ratio of the  $3d_{5/2}$  and  $3d_{3/2}$  is calculated to be 0.65 which is agreeing well with the theoretical value 0.66 for the ratio of 3d doublet. Presence of Cd in  $Cd^{1+}$  state confirms oxygen deficiency which is responsible for the better electrical conductivity of CdO thin films which is also seen in resistivity measurements [27].

### 3.5 Optical properties

The Yb:CdO films deposited by SPT have been investigated for optical absorption in the visible range using UV-Vis spectrophotometer. As the examination has been performed on film deposited on glass substrate, it is necessary to take into account the absorption by glass substrate on which films are formed. Hence the absorption spectra of glass substrate are also taken. Transmittance spectra of 2.5 at.% Yb:CdO film is shown in Fig. 6, transmittance of 81% measured at 550 nm and for all other Yb:CdO films, their transmittance values are mentioned in Table 2. It is found that the value of transmittance lies in the range of 74–81%. The increase in transmittance might be attributed to the well crystallized films and pinhole free surface. The optical band gap value are obtained from the following relation [28]

$$(\alpha h\nu) = A(h\nu - E_g)^n \quad (4)$$

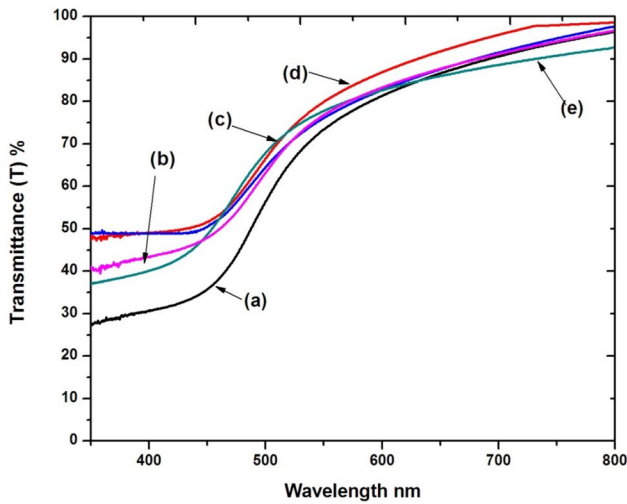


**Fig. 6** Transmittance of 2.5 at.% Yb:CdO thin film deposited at optimized substrate temperature of 350 °C

where  $\alpha$  is the absorption coefficient,  $h\nu$  is the photon energy,  $A$  is the constant and  $E_g$  is the optical band gap. The optical band gap values are determined from Tauc plot i.e.  $(\alpha h\nu)^2$  versus  $(h\nu)$  graph and extrapolating the linear portion of the graph on  $h\nu$  axis at  $\alpha = 0$ , as shown in Fig. 7. The values of direct band gap of Yb:CdO it increase from 2.63 to 2.88 eV as the Yb doping concentration increases for 1–2.5 at.% Yb:CdO films and further it is decreased to 2.77 eV. The increase in  $E_g$  value is attributed to increase in carrier concentration which leads to MB effect [29].

As per MB effect the increase in carrier concentration in degenerate semiconductors causes two opposite effects, namely the band gap widening (BGW) and band gap narrowing (BGN). The increase in optical band gap from 2.63 to 2.88 eV with the increase in Yb doping concentration is due to the blue shift of the absorption edge or is due to BGW which can be described by the MB effect, in which optical absorption edge of degenerate n-type semiconductor is shifted towards higher energy by amount proportional to the free electron density ( $n$ ) governing by following relation

$$BGW = \Delta E_g^{BM} = S_{BGW} N_{el}^{2/3} \tag{5}$$

$$S_{BGW} = \frac{\hbar^2}{2\gamma m_e} (3\pi^2)^{3/2} \tag{6}$$

where ‘ $\hbar$ ’ is the Planck’s constant and  $\gamma = m^*/m$  is the ratio for of reduced effective mass to free-electron mass, which is equal to 0.274 for pure CdO. Therefore, the value of the coefficient is  $S_{BGN} = 1.348 \times 10^{-14} \text{ eV cm}^2$ . The graph of  $\Delta E_g$  (i.e.  $E_g - E_{g0}$ ) versus  $n^{2/3}$  is plotted in Fig. 8. The best linear fit gives the value of  $S_{BGW}$  to be  $3.109 \times 10^{-14} \text{ eV cm}^2$ , which is nearly same as that of theoretical value, hence

**Table 2** The values of sheet resistance ( $R_s$ ), thickness ( $t$ ), transmittance ( $T$ ), figure of merit ( $\phi$ ), resistivity ( $\rho$ ), carrier concentration ( $n$ ), mobility ( $\mu$ ), Fermi energy ( $E_f$ ),  $n^{2/3}$ , mobility calculated, reflectivity (IR), and mean free path ( $l$ ) of 1–3 at.% Yb:CdO thin films deposited at 350 °C substrate temperature

Yb:CdO (at.%)	$R_s$ ( $\Omega$ )	$t$ (nm)	$T$ (%)	$\Phi$ ( $10^{-3} \Omega^{-1}$ )	$\rho$ ( $10^{-4} \Omega \text{ cm}$ )	$n$ ( $10^{20} \text{ cm}^{-3}$ )	$\mu$ ( $\text{cm}^2/\text{Vs}$ )	$E_f$ (eV)	$n^{2/3}$ ( $10^{13} \text{ cm}^{-2}$ )	$\mu$ cal ( $\text{cm}^2/\text{Vs}$ )	IR (%)	$l$ (nm)
1	5.75	746	74	8.56	7.2	3.91	25.05	1.04	5.34	18.37	94.15	27.35
1.5	3.45	897	77	21.23	4.2	6.86	21.98	1.51	7.77	12.63	96.43	22.68
2	3.10	1143	79	30.54	3.6	7.49	19.61	1.61	8.24	11.91	96.78	22.02
2.5	2.65	1375	81	45.87	2.6	13.9	17.39	2.43	1.24	7.88	97.24	17.92
3	2.75	1562	78	30.31	4.6	5.61	26.89	1.32	6.80	14.44	97.14	24.25

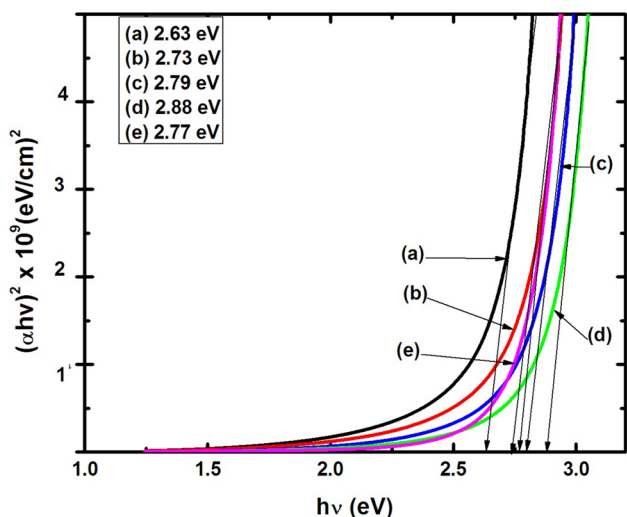


**Fig. 7** The plots of  $(\alpha hv)^2$  versus  $h\nu$  for Yb:CdO thin films of different Yb doping concentration deposited at substrate temperature of 350 °C

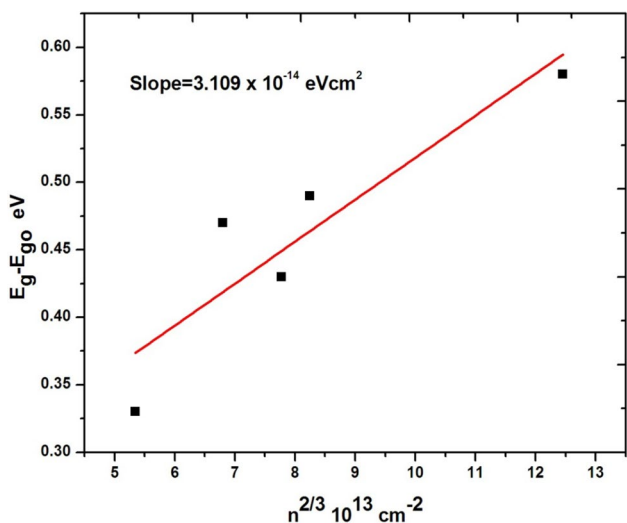


**Fig. 8** The BGW effect for Yb:CdO thin films deposited at 350 °C substrate temperature

observed band gap widening for Yb:CdO is due to MB effect. The difference might come from the non-parabolic band effects. The fact that the onset of light absorption is shifted towards lower wavelength in thin film turns out to be an advantage for optical applications in the near UV [29].

The TCOs having high reflectivity can be used in high quality solar window material, in flat panel collectors to conserve the heat etc. The IR reflectivity (R) of material is calculated using the following equation,

$$R = (1 + 2\epsilon_o \epsilon_o R_{sh})^{-2} \tag{7}$$

where  $R_s$  is the sheet resistance and  $1/2\epsilon_o \epsilon_o = 371$  is called impedance of free space. The IR reflectivity calculated for Yb:CdO films are in the range of 94.15–97.24% which are comparably very high than other TCOs reported [24]. The maximum reflectivity of 97.24% achieved for 2.5 at.% Yb:CdO film.

### 3.6 Electrical properties

The achievement of lowest possible resistivity is of practical significance as it provides freedom in selecting the thickness of film for achieving high optical transmission while maintaining the low resistivity. The electrical properties of metal oxide films depend critically upon the oxidation state of metallic component and on the type of impurities added in the films. The films with perfect stoichiometry are either insulators or ionic conductors. The electric properties of metal oxides can be improved by addition of suitable dopant of same or smaller ionic radii than that of host ion so it can be easily replaced without making any impurity oxide phases in film.

The variation of electrical resistivity ( $\rho$ ), carrier concentration ( $n$ ) and mobility ( $\mu$ ) measured at room temperature by four point probes Hall method in standard van der Pauw configuration and their values are tabulated in Table 2. As Yb doping concentration in CdO film increases, the resistivity decreases from  $7.2 \times 10^{-4}$  to  $2.6 \times 10^{-4} \Omega \text{ cm}$  for 2.5 at.% Yb:CdO film that is attributed to increase in carrier concentration. The Yb<sup>3+</sup> doped in CdO film replaces the Cd<sup>2+</sup> ions and thereby generates free electrons and increases the carrier concentration. The eventual increase in resistivity for 3 at.% Yb:CdO thin film to  $4.1 \times 10^{-4} \Omega \text{ cm}$  may be due to the fact that when Yb exceeds the limit of maximum solubility in CdO, it produces a grain boundary segregation of impurities which causes a dispersion of carriers leading to increase in resistivity. The mobility of Yb:CdO film decreases with increase in Yb concentration in CdO film from 25.05 to 17.39 cm<sup>2</sup>/Vs, this is due to increase in carrier concentration and decrease in resistivity. The increases in mobility can also be attributed to the decrease in grain boundary potential due to increase in grain size. Further the mobility is increased to 26.86 cm<sup>2</sup>/Vs for 3 at.% Yb:CdO film which may be due to decrease in grain boundary scattering. A high carrier concentration of  $13.9 \times 10^{20} \text{ cm}^{-3}$  is observed for 2.5 at.% Yb:CdO film. The variation of carrier concentration and mobility with increasing Yb doping in CdO thin film is plotted and shown in Fig. 9.

The film degeneracy is confirmed by evaluating Fermi energy using following relation

$$E_f = \left( \frac{h^2}{8m^*} \right) \left( \frac{3n}{\pi} \right)^{2/3} \tag{8}$$

where  $m^*$  is the value of effective mass = 0.21  $m_e$  in case of CdO film.



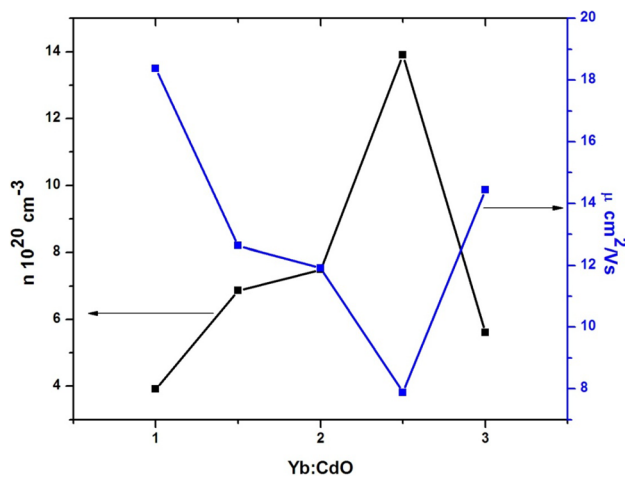


**Fig. 9** Variation of carrier concentration and mobility of Yb:CdO thin films of different Yb doping (1–3 at.%) deposited at 350 °C substrate temperature

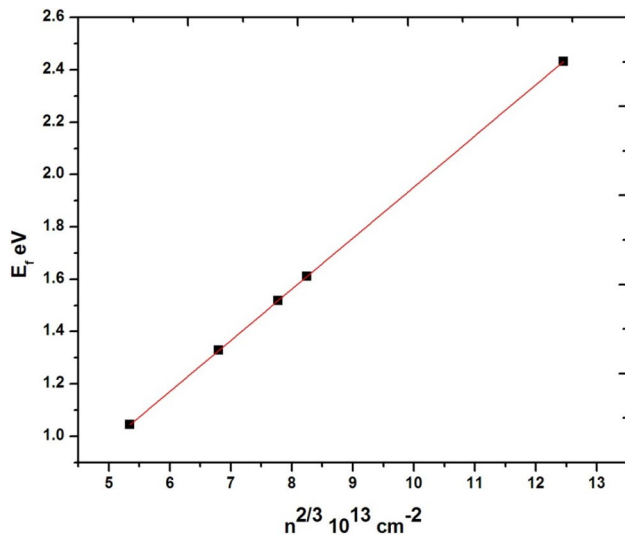


**Fig. 10** Variation of Fermi energy with respect to carrier concentration

The calculated Fermi energy is in the range of 1.04–2.43 eV. Further the Fermi energy values are proportional to  $n^{2/3}$  that is the characteristic of degenerate semiconducting material. As seen from Fig. 10 the plot is linear, from which it is concluded that the Yb:CdO films has degenerate semiconducting nature.

It is well known that in TCO thin films free carriers may interact with the different scattering centers. These centers may be the thermal vibrations of the lattice, the ionized or neutral impurities and the grain boundary regions. In polycrystalline semiconductor thin films the influence of

grain boundary has taken into account in addition to above scattering. For degenerate semiconductors the scattering by neutral impurity is not very much significant then in case of TCO the main scattering mechanism responsible for variation in mobility and other related parameters are ionized impurity scattering and grain boundary scattering. When the mean free path ( $l$ ) of the free carriers is comparable to the crystallite size the grain boundary scattering is dominant for the degenerate TCO films. The mean free path is obtained by the following relation

$$l = \left(\frac{h}{2e}\right) \left(\frac{3n}{\pi}\right)^{1/3} \cdot \mu \quad (9)$$

The values of the ‘ $l$ ’ calculated for 1–3 at.% Yb:CdO films and are depicted in Table 2 are in the range of 17.92–27.35 nm and the crystallite size ( $D$ ) estimated are in the range of 34.16–48.94 nm. Therefore it is clear that the ‘ $l$ ’ values are not comparable to ‘ $D$ ’ values and hence the grain boundary scattering mechanism is not dominant. Whereas the calculated theoretical values of mobility and experimental mobility values show similar trend and nearly equal values therefore it can be concluded that the ionized impurity scattering is the dominant mechanism for Yb:CdO films.

From application point of view of transparent conducting oxide in optoelectronic devices figure of merit ( $\Phi$ ) is one of the very important parameter. The variation of figure of merit with increasing Yb doping is calculated from Haacke’s formula [30]

$$\Phi = \frac{T^{10}}{R_s} \quad (10)$$

where  $T$  is transmittance and  $R_s$  is the sheet resistance. The figure of merit values of Yb:CdO thin films presented in Table 2. The values of sheet resistance decrease with increase in Yb doping concentration from 5.75 to 2.65  $\Omega$  and further increases to 2.75 for 3 at.% Yb:CdO film. The variation of figure of merit and sheet resistance is shown in Fig. 11 with increasing Yb doping concentration in CdO thin films. The figure of merit increases with Yb doping concentration from  $8.56 \times 10^{-3} \Omega^{-1}$  for 1 at.% Yb :CdO film and it is obtained maximum for 2.5 at.% Yb:CdO film is  $45.87 \times 10^{-3} \Omega^{-1}$  due to its high transmittance and low sheet resistance. Further it decrease to  $30.31 \times 10^{-3} \Omega^{-1}$  for 3 at.% Yb:CdO film. The possible explanation of it is due to variation of sheet resistance with increase in Yb doping shows opposite trend to figure of merit, first it decreases from 5.65 to 2.65  $\Omega$  and then it slightly increases to 2.75  $\Omega$  for 3 at.% Yb:CdO film. It also indicates the limiting solubility of Yb in host material is 3 at.%. The improved optoelectrical properties of Yb:CdO films are highly desirable in optoelectronic applications.

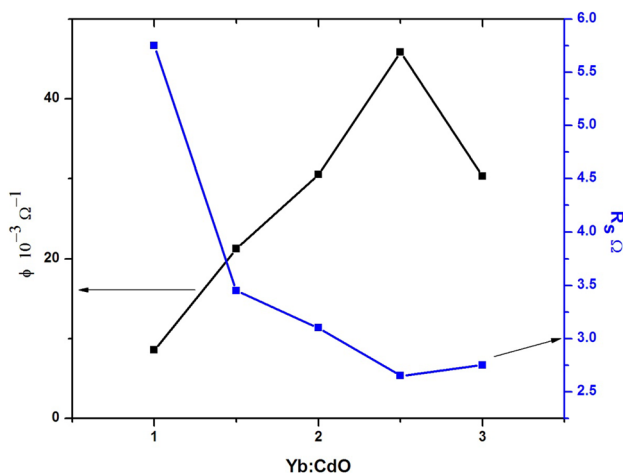


**Fig. 11** Variation of figure of merit and sheet resistance of Yb:CdO thin films deposited at optimized substrate temperature of 350 °C

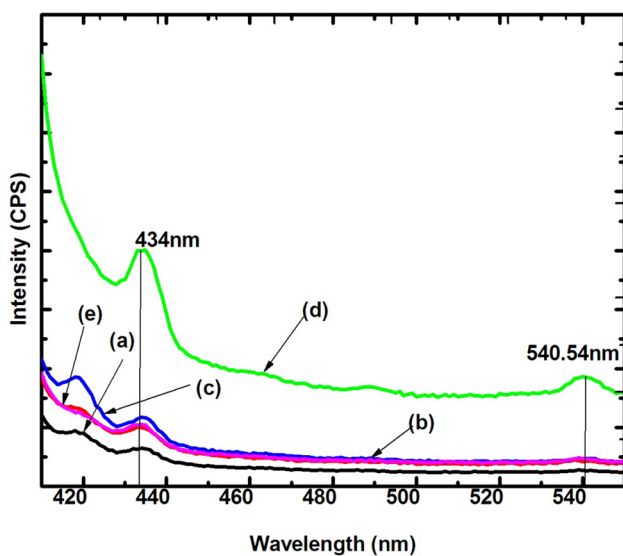


**Fig. 12** PL spectra of Yb:CdO films of different Yb doping (1–3 at.%) deposited at 350 °C substrate temperature

### 3.7 Photoluminescence (PL) studies

The room temperature PL spectrum of 1–3 at.% Yb:CdO thin films deposited at 350 °C substrate temperature is shown in Fig. 12. For the 2.5 at.% Yb:CdO film significant luminescent peaks are observed at 434 and 540.54 nm after excitation of films at 400 nm. It is observed that the peak position is shifted to higher energy side with the increase in Yb doping concentration in CdO film. It is possibly due to increase in film thickness. Moholkar et al. [29] also reported such kind of shift in wavelength with thickness for Ga doped CdO. The other possible reason was given for such kind of change by Shaleev et al. [31] who reported the PL shift

to higher energy side is attributed to increase in offset of valence band at the interface between island and deposited layer. Further it is also correlated with the surface morphological change with the increase in doping concentration of Yb which is observed in FE-SEM images and XRD results [32].

## 4 Conclusions

Yb doped CdO thin films have been successfully deposited on glass substrate using simple and cost effective SPT. XRD results showed that Yb:CdO thin films are polycrystalline face centered cubic in nature with preferred film orientation along (111) and (200) plane. Among these planes all the Yb:CdO films are strongly oriented along (200) plane. The other parameters like intensity, crystallite size, strain developed, dislocation density from (111) and (200) planes confirm that the Yb:CdO film with 2.5 at.% deposited at 350 °C temperature is optimized. The FE-SEM micrographs shows the densely packed and roughly spherical crystallites of Yb:CdO thin films. The band gap increases from 2.63 to 2.88 eV and further decrease to 2.77 eV with increase in Yb doping which is correlated to MB effect. The graph of  $\Delta E$  against  $n^{2/3}$  shows the variation in optical properties of film are related to the BGW phenomenon based on MB effect. The maximum reflectivity of 97.24% achieved for 2.5 at.% Yb:CdO film. The 2.5 at.% Yb:CdO film shows least electrical resistivity of  $2.6 \times 10^{-4} \Omega \text{ cm}$ , maximum carrier concentration of  $13.95 \times 10^{20} \text{ cm}^{-3}$ , mobility of  $17.39 \text{ cm}^2/\text{Vs}$ , lowest sheet resistance of  $2.65 \Omega$  and highest figure of merit of  $45.87 \times 10^{-3} (\Omega)^{-1}$  amongst all Yb:CdO thin films. PL study shows two emission peaks at 434 and 540.54 nm (green) and shift in peak position to higher energy side with the increase in Yb doping concentration in CdO films. These improved opto-electrical properties of Yb:CdO films makes it suitable candidate for opto-electronic based device fabrications.

## References

1. B.J. Ingram, G.B. Gonzalez, D.R. Kammler, M.I. Bertoni, T.O. Mason, Chemical and structural factors governing transparent conductivity in oxides. *J. Electroceram.* **13**, 167 (2004)
2. K. Hayashi, S. Matsuishi, T. Kamiya, M. Hirano, H. Hosono, Light-induced conversion of an insulating refractory oxide into a persistent electronic conductor. *Nature* **419**, 462 (2002)
3. T. Minami, Transparent conducting oxide semiconductors for transparent electrodes. *Semicond. Sci. Technol.* **20**, 35 (2005)
4. G. Lewis, C. David, B. Paine, Applications and processing of transparent conducting oxides. *MRS Bull.* **25**, 22 (2000)
5. R.G. Gordon, Criteria for choosing transparent conductors. *MRS Bull.* **25**, 52 (2000)

6. S.P. Desai, M.P. Suryawanshi, S.M. Bhosale, J.H. Kim, A.V. Moholkar, Influence of growth temperature on the physico-chemical properties of sprayed cadmium oxide thin films. *Ceram. Int.* **41**, 4867 (2015)
7. P.H. Jefferson, S.A. Hatfield, T.D. Veal, P.D.C. King, C.F. McConvillea, Bandgap and effective mass of epitaxial cadmium oxide. *Appl. Phys. Lett.* **92**, 022101 (2008)
8. Z. Zhao, D.L. Morel, C.S. Ferekides, Electrical and optical properties of tin-doped CdO films deposited by atmospheric metalorganic chemical vapor deposition. *Thin Solid Films* **413**, 203 (2002)
9. A.A. Dakhel, Bandgap narrowing in CdO doped with europium. *Opt. Mater.* **31**, 691 (2009)
10. A.A. Dakhel, Transparent conducting properties of samarium-doped CdO. *J. Alloys Compd.* **475**, 51 (2009)
11. A.A. Dakhel, Correlated transport and optical phenomena in Ga-doped CdO films. *Sol. Energy* **82**, 513 (2008)
12. A.A. Dakhel, Influence of hydrogenation on the electrical and optical properties of CdO:Tl thin films. *Thin Solid Films* **517**, 886 (2008)
13. A.A. Dakhel, Electrical and optical properties of iron-doped CdO. *Thin Solid Films* **518**, 1712 (2010)
14. A.A. Dakhel, Structural and optoelectrical properties of nanocrystalline Gd-doped CdO films prepared by sol gel method. *J. Sol-Gel Sci. Technol.* **55**, 348 (2010)
15. F.C. Eze, Oxygen partial pressure dependence of the structural properties of CdO thin films deposited by a modified reactive vacuum evaporation process. *Mater. Chem. Phys.* **89**, 205 (2005)
16. A.J. Varkey, A.F. Fort, Transparent conducting cadmium oxide thin films prepared by a solution growth technique. *Thin Solid Films* **239**, 211 (1994)
17. B. Saha, S. Das, K.K. Chattopadhyay, Electrical and optical properties of Al doped cadmium oxide thin films deposited by radio frequency magnetron sputtering. *Sol. Energy Mater. Sol. Cells* **91**, 1692 (2007)
18. A.V. Moholkar, G.L. Agawane, K.-U. Sim, K.Y. Ye-bin Kwon, J.H. Rajpure, Kim, Influence of deposition temperature on morphological, optical, electrical and opto-electrical properties of highly textured nano-crystalline spray deposited CdO:Ga thin films. *Appl. Surf. Sci.* **257**, 93 (2010)
19. L.R. de León-Gutiérrez, J.J. Cayente-Romeroa, J.M. Peza-Tapiaa, E. Barrera-Calvab, J.C. Martínez-Floresb, M. Ortega-López, Some physical properties of Sn-doped CdO thin films prepared by chemical bath deposition. *Mater. Lett.* **60**, 3866 (2006)
20. A. Gulino, P. Dapporto, P. Rossi, I. Fragala, Synthesis and characterization of liquid MOCVD precursors for thin films of cadmium oxide. *Chem. Mater.* **14**, 4955 (2002)
21. R.K. Gupta, K. Ghosh, R. Patel, S.R. Mishra, P.K. Kahol, Preparation and characterization of highly conducting and transparent Al doped CdO thin films by pulsed laser deposition. *Curr. Appl. Phys.* **9**, 673 (2009)
22. S.P. Desai, M.P. Suryawanshi, M.A. Gaikwad, A.A. Mane, J.H. Kim, A.V. Moholkar, Investigations on the thickness dependent structural, morphological, and optoelectronic properties of sprayed cadmium based transparent conducting oxide. *Thin Solid Films* **628**, 196 (2017)
23. P. Scherrer, *Göttinger Nachrichten Gesell*, vol **2**. (Springer, Berlin, 1918), p. 98
24. A.V. Moholkar, S.M. Pawar, K.Y. Rajpure, C.H. Bhosale, J.H. Kim, Effect of fluorine doping on highly transparent conductive spray deposited nanocrystalline tin oxide thin films. *Appl. Surf. Sci.* **255**, 9358 (2009)
25. A.A. Yadav, Influence of film thickness on structural, optical, and electrical properties of spray deposited antimony doped SnO<sub>2</sub> thin films. *Thin Solid Films* **591**, 18 (2015)
26. K. Gurumurugan, D. Mangalaraj, K. Narayandass, Structural characterization of cadmium oxide thin films deposited by spray pyrolysis. *J. Cryst. Growth* **147**, 355 (1995)
27. S.W. Gaarenstroom, N. Winograd, Initial and final state effects in the ESCA spectrum of cadmium and silver oxide. *J. Chem. Phys.* **67**, 3500 (1977)
28. R. Nyholm, N. Martensson, Experimental core-hole ground state energies for the elements <sup>41</sup>Nb to <sup>52</sup>Te. *Solid State Commun.* **40**, 311 (1981)
29. A.V. Moholkar, G.L. Agawane, K.-U. Sim, Y. Kwon, D.S. Choi, Temperature dependant structural, luminescent and XPS studies of CdO: Ga thin films deposited by spray pyrolysis. *J. Alloys Compd.* **506**, 794 (2010)
30. G. Haacke, New figure of merit for transparent conductors. *J. Appl. Phys.* **47**, 4086 (1976)
31. M.V. Shaleev, A.V. Novikov, A.N. Yablonskii, O.A. Kuznetsov, Yu.N. Drozdov, D.N. Labnov, Z.F. Krasilnik, *J. Semicond.* **41**, 1356 (2007)
32. G. Mumoita, C.N.R. Rao, Solvothermal synthesis of CdO and CuO nanocrystals. *Chem. Phys. Lett.* **393**, 493 (2004)